JOINT EUROPEAN TORUS

JET–P(93)71

B. Balet, D.V. Bartlett, J.G. Cordey, R. König, H. W Morsi,
D.P. O’Brien, P. Smeulders, D. Stork

Energy Transport during the Pellet Enhanced Performance (PEP) Discharges in JET

Energy Transport during the Pellet Enhanced Performance (PEP) Discharges in JET

B. Balet, D.V. Bartlett, J.G. Cordey, R. König, H.W. Morsi,
D.P. O'Brien, P. Smeulders, D. Stork

JET-Joint Undertaking, Culham Science Centre, OX14 3DB, Abingdon, UK

Preprint of a paper to be submitted for publication in the Proceedings of
Varenna Workshop on 'Local Transport Studies in Fusion Plasmas'
(Varenna, 30 August 1993)
September 1993

I. INTRODUCTION

A transient enhancement in the performance of JET discharges was first obtained in the L-mode regime when a peaked density profile formed by pellet injection was heated using Ion Cyclotron Resonance Heating (ICRH) alone [1]. The enhancement of the central parameters observed in such modes was later combined with the edge related enhancement obtained in the H-mode regime and was achieved with combined ICRH and Neutral Beam Injection (NBI) heating [2]. Since then Pellet Enhancement Performance (PEP) modes have been created in a number of discharges at various plasma conditions (I_p = 1 to 4.1 MA; B_T = 2.2 to 3.5T; heating methods varying from up to 16 MW ICRH to 18 MW NBI). Several PEP discharges have been analysed using the TRANSP code [3] to try and establish the reason for the good performance and to assess the effects of the different heating schemes.

The main experimental measurements given as input to the TRANSP code are as described elsewhere [4]. The profiles of the electron temperature T_e (from Electron Cyclotron Emission measurements) and electron density n_e (from far infra-red measurements) were cross-checked by LIDAR Thomson scattering measurements. For the discharges with pellet injection, the electron density profiles are very peaked and their shapes are more accurately determined by the LIDAR measurements. In order to carefully reproduce the time evolution of these PEP discharges, electron density data combining the radial definition of the LIDAR measurements with the time evolution of the far infra-red diagnostics was given as input to the code. The high density values achieved in these PEP discharges ($n_e(o) \lesssim 10^{20}$ m^{-3}) led to central ion temperatures measured by the high resolution X-ray spectrometer equal or slightly higher than the central electron temperatures; the ion temperature T_i was therefore assumed to have the same profile shape as the electron temperature T_e. The high density of these pulses also meant that the ion and electron channels in the power balance are difficult to separate. Therefore, this paper will only discuss the characteristics of an effective heat conductivity χ_{eff} defined by (total conduction)/($n_e\nabla T_e + n_i\nabla T_i$).

The paper is divided into five sections. In Section II, the comparison of a PEP versus a no-PEP discharge is presented. Section III deals with the effects of the different heating schemes in the PEP regime. The possible reasons for the good central confinement of these PEP discharges are investigated in Section IV. Finally a summary and conclusions are presented in Section V.

II. COMPARISON OF PEP VERSUS NO-PEP DISCHARGES

Two nearly identical NBI heated discharges have been analysed. In one of them a pellet was fired (the PEP discharge) whereas in the other no pellet was injected (the no-PEP discharge). The main characteristics of these two pulses are shown in Fig. 1. Both discharges are 3 MA, 3.4T H-modes with some 13 MW of D° beam injection. A 4 mm pellet fired into one of the discharges creates a peaked density profile ($n_e(o)/\langle n_e \rangle \approx 3.2$ at 5s) which lasts for ~ 1s. The density profiles for these two pulses are compared in Fig. 2: both discharges show an edge pedestal characteristic of the H-mode; the PEP discharge exhibits high central value and steep gradient over the central 60 cm of the plasma (the PEP region). The higher central density of the PEP discharge leads to higher diamagnetic energy and neutron emission rate than in the no-PEP discharge. The TRANSP simulations of these two pulses show that ~ 75% of the total neutron yield is from beam-thermal reactions.

In the power balance obtained from TRANSP, the main loss is through conduction; the convection loss is small in the centre and only becomes significant near the edge. The derived effective heat conductivity profiles χ_{eff} are shown in Fig. 3 for the two pulses at the time of the LIDAR measurements. For the PEP discharge, with steep density gradients in the core of the plasma, the central confinement is improved compared to the "normal" no-PEP H-mode. In the centre, χ_{eff} (PEP) $\simeq 1\ m^2/s$; whereas χ_{eff} (no-PEP) $\simeq 1.7\ m^2/s$.

III. PEP DISCHARGES WITH DIFFERENT HEATING SCHEMES

PEP discharges with pure NBI or ICRH achieved the same fusion power at similar levels of plasma energy. However, it appeared that PEP discharges with predominantly NBI heating and a small amount of ICRH gave the highest neutron yield [5]. This seemed to suggest the existence of synergetic effects of the ICRH such as for example the acceleration of the fast beam ions by the waves. To investigate that issue, a TRANSP analysis of two similar 2.8T, 3MA PEP + H-mode discharges has been performed. In both cases, 11.5 MW of NBI is applied at the time of the pellet injection. In one discharge, 3.2 MW of ICRH is combined with the NBI heating. Whereas the electron density profiles are very similar for both discharges, the electron temperature profiles are different (see Fig. 4a): the central electron temperature increases from ~ 5 keV to ~ 7 keV and the region of enhanced confinement is broader in the pulse with combined heating. Clearly the electron temperature responds to the increased central heating (see Fig. 4b).

The power balance of these two discharges has the same characteristics as described in Section II. The effective heat conductivities χ_{eff} are very similar for both cases. The dominant effect of the ICRH is that the power penetrates the plasma core even at high density: some 90% of the total ICRH power is deposited in the central half of the plasma. This is in marked contrast to the NBI case where only 50% of the total power is deposited in the centre (see Table I). Hence the TRANSP analysis shows that no synergetic effects due to ICRH are needed to explain the better performances obtained with combined heating.

IV. POSSIBLE EXPLANATIONS FOR THE ENHANCED CONFINEMENT IN THE PEP REGION.

Fig. 3 shows that the improvement in the confinement of the PEP + H-mode relative to an ordinary H-mode occurs in the core of the plasma ($\rho \leq 0.5$). The TRANSP analysis shows that the particle transport is also reduced in the central region relative to its edge value and has a radial dependence similar to impurity transport in L-mode [6]; this explains the maintenance of the peaked density profile throughout the PEP phase.

For the PEP discharge, Fig. 5 shows a strong off-axis bootstrap current which is mainly driven by the large density gradient in the PEP core; it gives rise to a negative shear in the central region of the PEP discharges (see Fig. 6). The off-axis bootstrap current has been found to reach values of $1MA/m^2$ in PEP pulses with combined heating. A minimum q is achieved near the position of the maximum bootstrap current density. The presence of this non monotonic q profile is further confirmed by MHD observations, magnetic equilibrium reconstruction (EFIT-J), Faraday rotation diagnostics and analysis of soft X-ray data [7]. Regarding the stability of ideal ballooning modes, a value of minimum $q \geq 1.19$ gives access to the second stable region and therefore the negative shear region of the PEP discharges increases the volume which is ballooning stable, and could explain the good central confinement. A full stability analysis is in progress Furthermore the Rebut, Lallia, Watkins scaling [8] has suggested an enhanced confinement if $\nabla q < o$ (in such cases, the anomalous transport is switched off) and a satisfactory simulation of PEP discharges is obtained with the RLW model [7]. Other possible correlations of χ_{eff} have been investigated; this is illustrated in Fig. 7 where the

χ_{eff} profiles of the PEP and no-PEP discharges are compared with the corresponding profiles of $1/n_e$, $\eta_{ie} = (n_i/\nabla n_i)/(T_i/\nabla T_i)$ and the shear $s = (r/q)(dq/dr)$. The region of negative shear is smaller than the region of reduced transport for the PEP discharge. The stabilisation of η_i mode by the peaked density profile or the correlation of χ_{eff} with $1/n_e$ (Alcator like scaling) appear to be possible explanations of the good central confinement of the PEP discharge. However attempts to correlate the time evolution of χ_{eff} with η_{ie} and $1/n_e$ are less convincing. Furthermore, it has been shown that η_i-mode theory fails to reproduce JET data [9, 10].

V. SUMMARY AND CONCLUSIONS

A transient enhancement of the central plasma parameters is observed in pulses where a pellet is injected early in the discharge prior to the occurrence of the $q = 1$ surface in the plasma and to the onset of a strong auxiliary heating. PEP discharges have been obtained in L-and-H-modes at various plasma conditions; they are all characterised by very peaked density profiles. The TRANSP analysis shows that the energy transport of the PEP discharges is reduced in the central region relative to a no-PEP discharge and that χ_{eff} is close to the neoclassical value in the core region. Central heating by ICRH leads to improved central electron and ion temperatures and enhanced fusion performance but χ_{eff} remains unchanged. The reasons for the good central confinement remain unclear, but it could be associated with a negative shear region in the core of the plasma driven by a strong off-axis bootstrap current. This leads to the stabilisation of ballooning modes and access to the second stability region. The stabilisation of η_i mode by the peaked density profile or the correlation of χ_{eff} with $1/n_e$ are also possible explanations.

REFERENCES

[1] The JET team, Proc. 12th IAEA Conf. Nice, 1988, Vol. 1, IAEA, Vienna (1989) 215.

[2] Tubbing, B.J.D., et al., Nucl. Fus. 31 (1991) 839.

[3] Goldston, R.J., et al., J. Comput. Phys. 43 (1981) 61.

[4] Balet, B., et al., Nucl. Fus. (1993, to be published).

[5] Bures, M., et al., Proc. 20th EPS Conf. 1993, 17C (I) p.171.

[6] Pasini, D., et al., Proc. 19th EPS, Conf. 1993, 16C (I) p.283.

[7] Hugon, M., et al., Nucl. Fus. 32 (1992) 33.

[8] Rebut, P.H., et al., Phys. Fluids (B) 3 (1992) 2209.

[9] Tibone, F., et al., Proc. 17th EPS Conf. 1990, 14B (III) p.805.

[10] Balet, B., et al. Plasma Phys. and Control. Fusion 34 (1) (1992) 3.

TABLE I t = 5.21s power deposited in the PEP region ($\rho < 0.5$)	PEP + NBI #26705	PEP + NBI, ICRH #26712
from NBI to electrons	1.55 MW	1.3 MW
from NBI to ions	3.85 MW	4.55 MW
from ICRH to electrons	-	1.1 MW
from ICRH to ions	-	1.8 MW
TOTAL	5.4 MW	8.75 MW

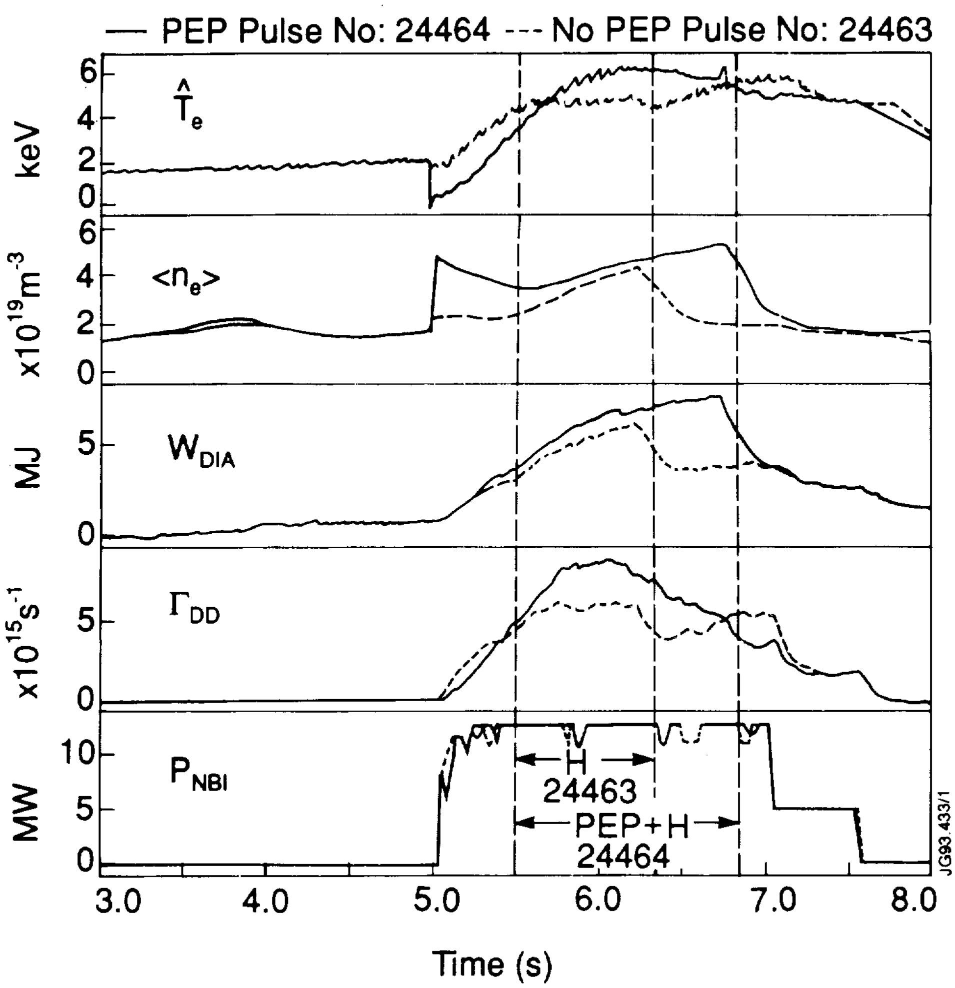

Fig. 1. The time evolution of the central electron temperature T_e, the volume-averaged electron density $<n_e>$, the plasma diamagnetic energy W_{DIA}, the total neutron rate Γ_{DD} and the neutral beam power P_{NBI} for a PEP pulse (solid line) and a no-PEP pulse (dotted line).

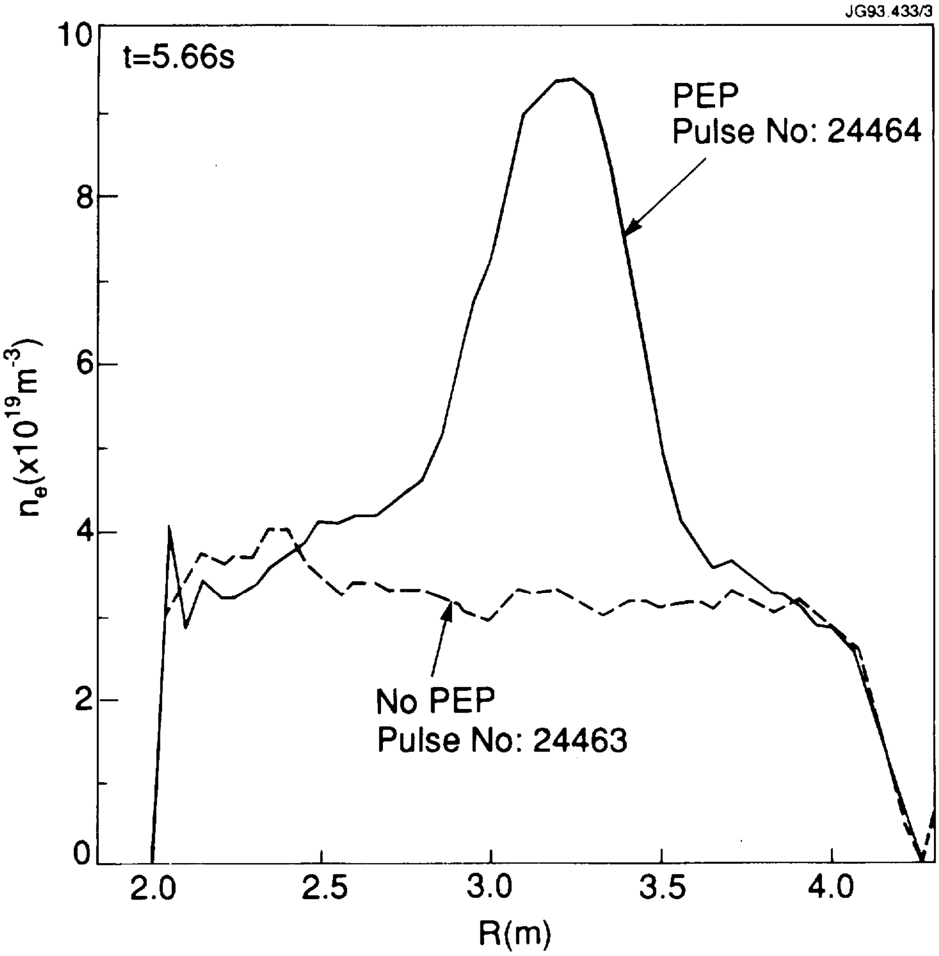

Fig. 2. Electron density profile from Lidar measurements at t = 5.66s for a PEP pulse (solid line) and a no-PEP pulse (dotted line).

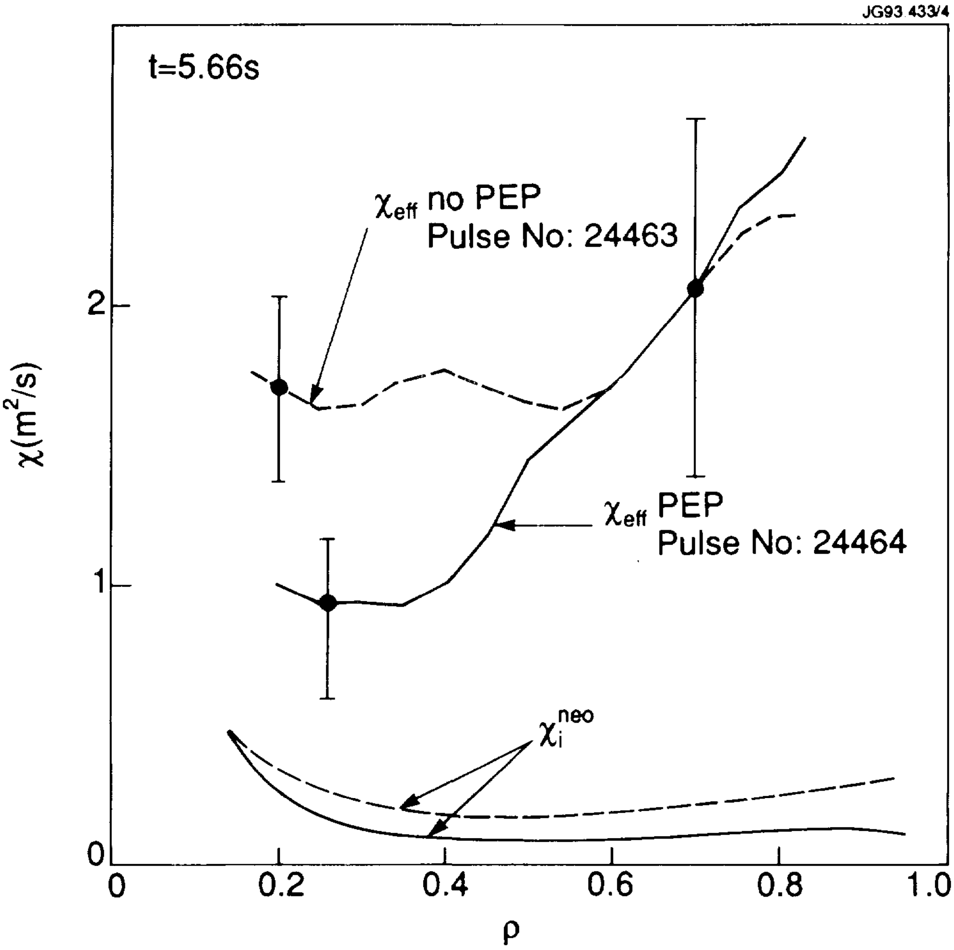

Fig. 3. Effective heat conductivity χ_{eff} and neoclassical values χ_i^{neo} versus normalised radius ρ for a PEP pulse (solid line) and a no-PEP pulse (dotted line).

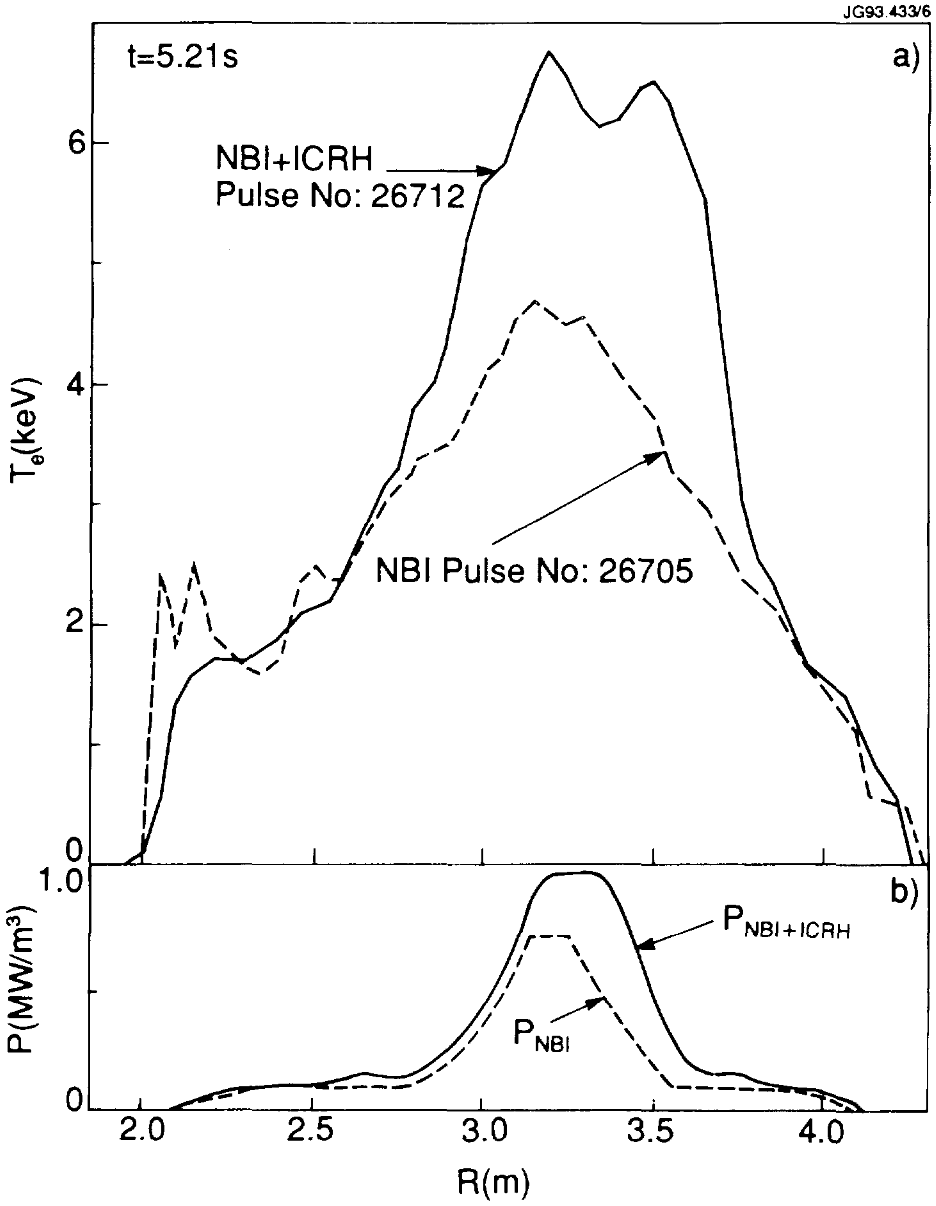

Fig. 4. a) Electron temperature profiles from Lidar measurements and b) Power deposition profiles for the NBI heated pulse (dotted line) and the pulse with combined heating (solid line) at t = 5.21s.

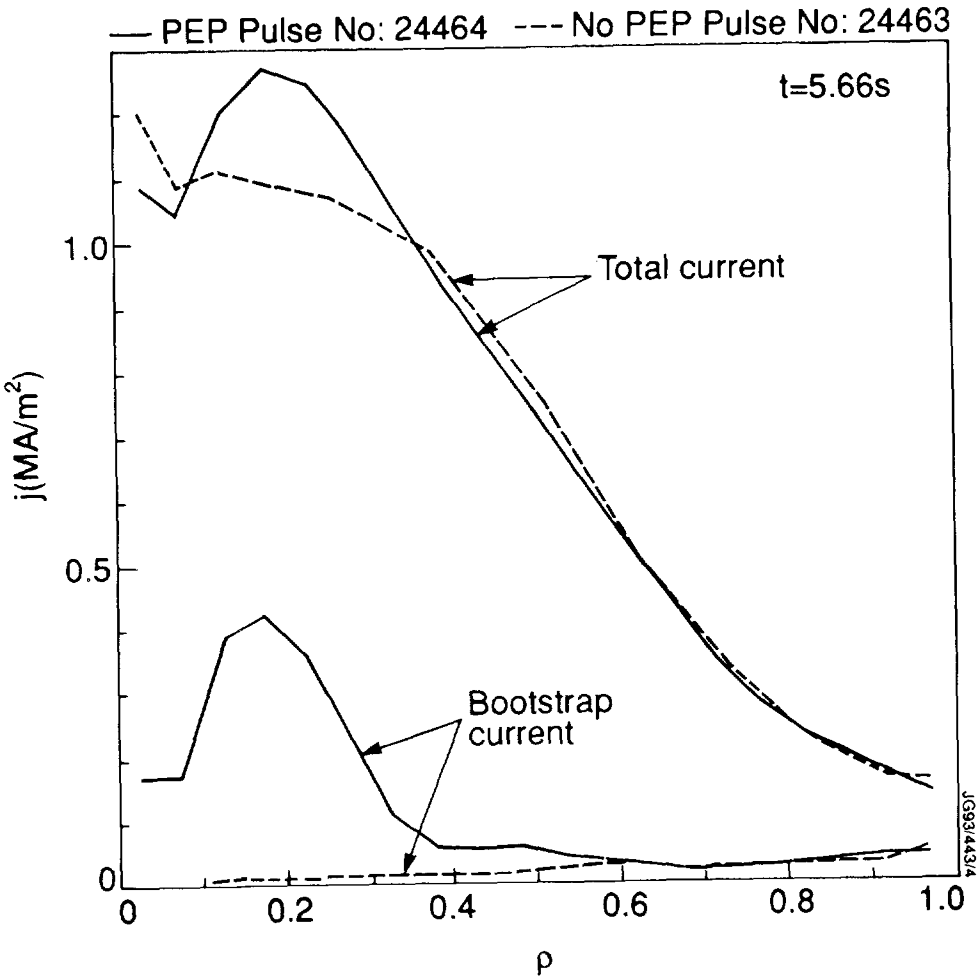

Fig. 5. The total and boostrap current densities versus ρ for a PEP pulse (solid line) and a no-PEP pulse (dotted line).

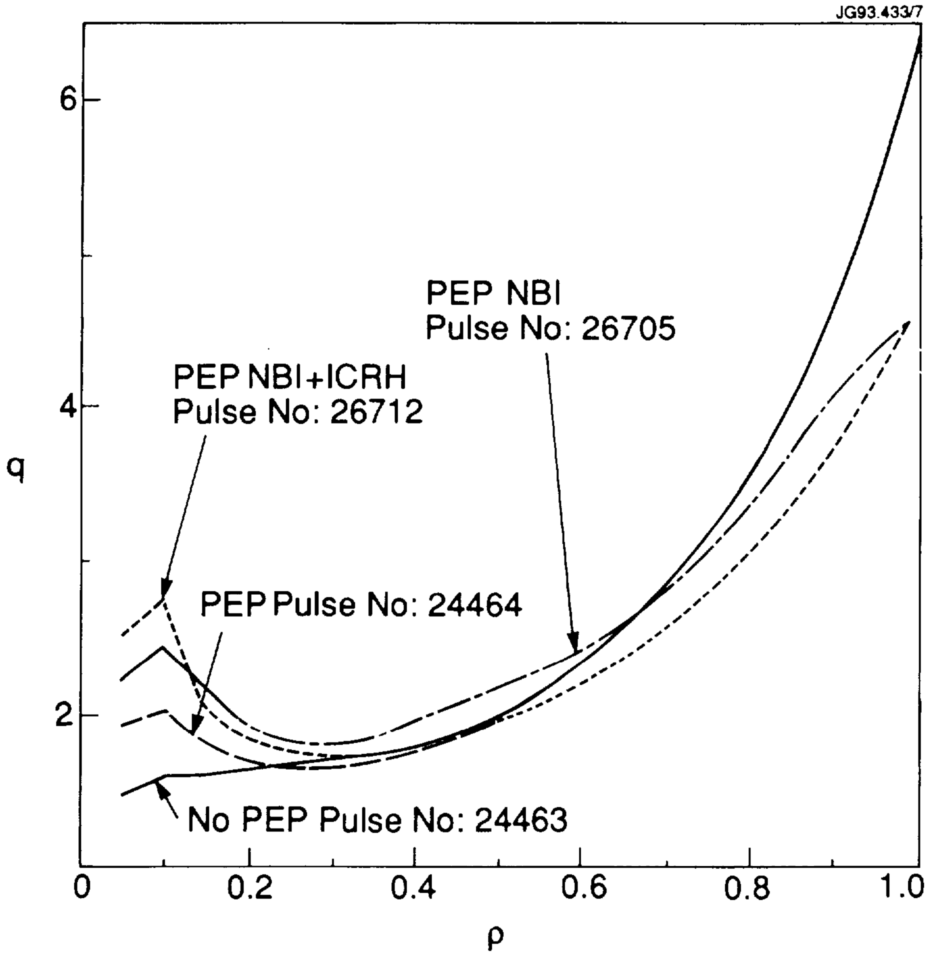

Fig. 6. q profiles versus ρ for PEP pulses and the no-PEP pulse.

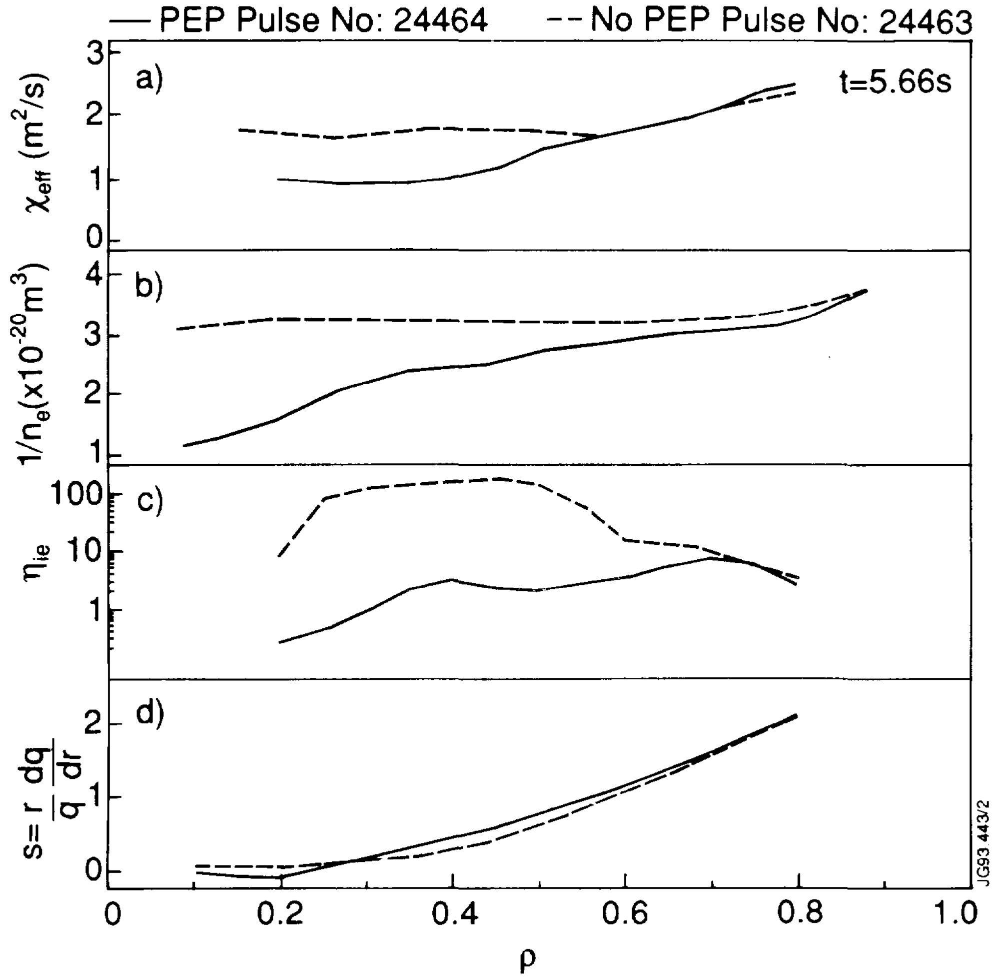

Fig. 7. The profiles of a) χ_{eff}, b) $1/n_e$, c) $\eta_{ie} = (n_e/\nabla n_e)/(T_i/\nabla T_i)$ and d) shear $s = (r/q)\,(dq/dr)$ versus ρ for a PEP pulse (solid line) and a no-PEP pulse (dotted line).